© Vladimir Timofeev | Dreamstime.com

Tree cover loss detection using optical and radar sensors

A case study from South Sumatera and East Kalimantan, Indonesia

RESTORE+

Working Paper

Tree cover loss detection using optical and radar sensors

A case study from South Sumatera
and East Kalimantan, Indonesia

International Institute for Applied Systems Analysis
Vienna, January 2022

Authors:

Adrian Dwiputra, University of British Columbia

Hadi, International Institute for Applied Systems Analysis

Neha Joshi, International Institute for Applied Systems Analysis

Steffen Fritz, International Institute for Applied Systems Analysis

Executive Summary

- We explored the potential of radar and optical remote sensing analysis to map tree cover loss in tropical forest landscapes in two provinces in Indonesia: South Sumatera (SS) and East Kalimantan (EK).

- Tree cover loss was mapped using three approaches: 1) optical satellite images, 2) radar data, and 3) the combination of optic-based and radar-based change maps using simple overlay between maps produced using 1) and 2).

- The optic-based change maps were produced using the Continuous Change Detection and Classification (CCDC), while the radar-based change maps were produced using the backscatter difference thresholding approach. Both optic-based and radar-based approaches were implemented in Google Earth Engine (Gorelick et al., 2017).

- Combining the optic-based map with the radar-based map yielded the best mapping accuracy values, suggesting that more sophisticated approaches to combine the two sensor types should be explored further, for example, by fusing the optical and radar data using machine learning algorithms, e.g., random forest (Breiman 2001).

Table of Contents

1. Introduction

Countries with high natural ecosystem cover play an important role in climate change mitigation and adaptation actions. In many cases, such as in Brazil and Indonesia, the natural ecosystems are under threat of anthropogenic disturbances. Irreversible ecosystem degradation often follows intensive disturbance events, such as massive deforestation and human-induced wildfires in tropical rainforests. Therefore, avoiding further deforestation and degradation while promoting ecosystem restoration is a pragmatic step to address the global climate and biodiversity crises.

As we observe an increase in the official commitments made by the world governments to reduce deforestation and ecosystem degradation over the last decade, systematic monitoring of the fulfilment of the pledges has never been more important. Essential resources required in the monitoring are maps that show the occurrence, location, and area of forest degradation and deforestation, which are often associated by the major loss of tree cover, in landscapes of interest. However, tree cover loss maps are not always available to support continuous monitoring of natural land cover. Data gaps are one of the major challenges in establishing a transparent monitoring system to monitor and verify the climate and biodiversity commitments.

Remote sensing can offer a potential solution to close the identified data gaps. However, the conventional tree cover loss mapping using optical satellite images often does not work as effectively in tropical landscapes as in other areas due to the persistent cloud cover. A potential solution to improve the tree cover loss mapping is by complementing the optical satellites images with radar satellites observations. The longer wavelengths used in radar remote sensing can penetrate clouds and thus allow data acquisition over landscapes of interest even in cloudy environments (Sabins 1997).

This report provides technical documentation of our attempt to map tree cover loss using radar and optical satellites in two provinces in Indonesia, namely South Sumatera and East Kalimantan. We aimed to contribute relevant empirical information to improve remote sensing techniques in mapping tree cover loss in the dynamic yet data-limited tropical forest landscapes.

1.1 Objectives

We explored the potential of radar and optical remote sensing analysis to map tree cover loss in the two study provinces in Indonesia, South Sumatera and East Kalimantan. Evaluating the accuracy and sensitivity of optical and radar remote sensing in mapping tree cover loss provides empirical information on the pros and cons of the two sensor types used, which will be valuable in determining the most effective approach to monitor land cover dynamics in data-limited tropical forest landscapes.

In the context of the RESTORE+ project, this study evaluates the proposed approach along with descriptions of technical steps for implementation. The aim is to allow relevant stakeholders/landscape managers to gain valuable technical insights to generate relevant land cover monitoring data that can be used in formulating and evaluating restoration strategies in their landscapes of interest.

2. Mapping tree cover loss using optical and radar remote sensing

2.1 Study Area

Indonesia is one of the tropical countries with the highest potential for carbon sequestration from avoided deforestation and forest degradation. The exceptionally high biodiversity in the country, with high endemism, is challenging to conserve due to anthropogenic pressures. For example, rapid forest conversions into agricultural lands are commonly found as the economy develops. The forest conversion releases a significant amount of greenhouse gas emissions, exacerbating global climate change, and contributes to biodiversity loss through habitat loss or degradation.

This study covers two provinces in Indonesia that hold environmental significance: South Sumatera (SS) and East Kalimantan (EK). The selected provinces are relatively advanced in terms of climate change mitigation and biodiversity conservation commitments. For instance, both provinces have formulated green economic growth action plans that incorporate environmental indicators in their economic development plans.

The landscapes of SS and EK are home to high-carbon stock natural forests, each with unique characteristics. A massive proportion of the carbon stock in SS is concentrated in the 1.3 million hectares of tropical peat swamp forest as below-ground organic matter and above-ground plant biomass (The Ministry of Environment and Forestry of Indonesia 2021). In contrast, EK has only 0.3 million hectares of peatland area, and thus, relatively smaller carbon is stored as below-ground peat (The Ministry of Environment and Forestry of Indonesia 2021). Natural land cover in the two provinces has been reduced in the recent decade, mostly due to increased land demand for economic activities such as plantations expansion, among other anthropogenic activities that affect the natural ecosystem intactness, such as timber extraction associated with both legal and illegal logging activities. Wildfires associated with fire used in land clearing activities exacerbate the natural ecosystem degradation in the two provinces (Dewi et al., 2015).

2.2 Methods

The analysis comprised change mapping using three approaches: 1) optical satellite images, 2) radar data, and 3) the combination of optic-based and radar-based change maps, as well as the evaluation of the produced maps.

The optic-based change maps were produced using the Continuous Change Detection and Classification (CCDC) algorithm developed by Zhu & Woodcock (2014). The algorithm implementation in Google Earth Engine (GEE; Gorelick et al., 2017) by the GEE team was used. The input was Normalized Difference Moisture Index (NDMI = (NIR-SWIR1)/(NIR+SWIR1)) dense time series calculated from all available clear-sky Landsat observations (F mask) from 1984 to 2019. The algorithm was run with the parameter of minimum consecutive anomalous observations to be flagged as land change equals six (6) observations to minimize the false-positive detection rate. (note for more

sensitive/less conservative detection, the fewer required number of consecutive anomalies, e.g. four or/and lower chi-square probability threshold, e.g. 0.90 for detection could be set, depending on validation results). Multitemporal cloud masking (T-mask) was not applied. The default values for the other parameters of the algorithm were used. Of the detected change events, only the events with negative change magnitude—indicating tree cover loss—were kept. Post-processing based on the size of contiguous change pixels was not yet applied.

The radar-based change maps were produced using the backscatter difference thresholding approach. We implemented the steps in Google Earth Engine (GEE) just like the optic-based change to standardize the framework. The inputs were ortho-rectified and terrain-corrected gamma naught backscatter data acquired by several radar satellites, namely Sentinel-1, ALOS-PALSAR/PALSAR-2. Since Sentinel-1 and ALOS-PALSAR/PALSAR-2 use different wavelengths in data acquisition, the data from the two different sources can be expected to have high complementarity since they capture the state of the observed landscapes differently. Sentinel-1 data are only available for the 2015-2018 analysis period as the mission began in late 2015.

In general, forests and other tree-dominated lands are associated with higher radar backscatter values. Therefore, significant reductions of backscatter values are associated with major tree cover loss as observed in the events of deforestation or forest degradation. The threshold of the backscatter reduction associated with tree cover loss events was determined using expert judgement following multiple trials of visual interpretations. Since radar data are associated with relatively high noise content, several masking and filtering procedures were applied to reduce the noise, such as the refined Lee filter, mask based on the Hansen global forest change map (Hansen et al. 2013), and terrain/topography-based mask. Among the applied filters, post-processing based on the size of contiguous change pixels was applied. Change patches composed of less than 60 spatially connected pixels were omitted.

Despite the variations in the spatial resolution of the different satellite data used in the analysis, all change maps were produced as rasters with 30-m pixel size. While the final raster resolution matches the optical satellite data's resolution, the radar data used originally have higher spatial resolutions. However, the high noise content in radar data was one of the main reasons why the radar-based maps were resampled into the coarser spatial resolution of 30-m.

We combined the change maps derived from the optic-based and radar-based approaches to create other maps. In the first combined map that we will refer to as "Optical-radar union", after we overlayed the optic-based with the radar-based change map, the pixels were assigned as "change" when at least one of the two maps detected a tree cover loss occurrence. In the second one ("Optical-radar intersection"), we only took the overlap between the optic-based and the radar-based change maps.

We evaluated the three produced maps (i.e., the optical-only, radar-only, and combined change maps) in terms of the overall accuracy, sensitivity, and specificity. The evaluation was conducted with reference data from a field survey conducted under the RESTORE+ Jelantara campaign and a desktop-based survey using CollectEarth software (Bey et al. 2016). Through Jelantara campaign, hundreds of geographic points in South Sumatera were surveyed, 208 of which were used as part of the reference

data for the change map validation. Many surveyed points were filtered out due to the low confidence of the collected information.
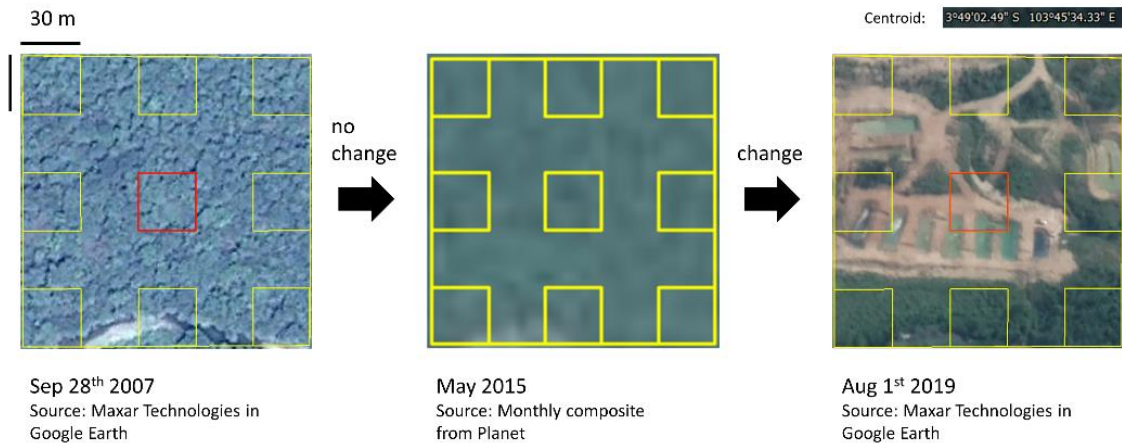

Figure 2.1 An example of very-high resolution satellite images interpretation in Collect Earth

The majority of the reference data were collected through the interpretation of very-high-resolution satellite images in CollectEarth software. CollectEarth provided simultaneous access to different platforms that hosted high-resolution satellite images, which were observed to detect any occurrences of tree cover loss within the studied periods. The sampling design implemented was a combination of random points and cluster sampling to maximize the point collection. First, the centroids of the sampling cluster were distributed in a stratified random manner based on the combined change maps in *Area2* GEE tool, which targeted overall accuracy's standard error of 0.018. The other 8 points were then spread around the centroid with the spacing of at least 30 meters (1-pixel side length) to maintain independence between each of the points. While the assignment of the values of change/no change was conducted per point, most of the points in the clusters were found to have experienced the same change, probably due to the large scale of the changes in the observed landscapes. The total number of reference data used in the evaluation is provided in the following table.

Table 2.1 Reference points used in results evaluation

| Province | Period | Number of Points | |
		change	no-change
East Kalimantan	2010-2015	198	216
East Kalimantan	2015-2018	153	351
South Sumatera	2010-2015	216	469
South Sumatera	2015-2018	207	487

Reference

	No change	Change	
Result map No change	True negative (TN)	False negative (FN)	Negative Predictive Value (NPV) = TN/(FN+TN)
Change	False positive (FP)	True positive (TP)	User's accuracy (UA) = TP/(FN+TN)
	True negative rate (TNR) = TN/(FP+TN)	Producer's accuracy (PA) = TP/(TP+FN)	

Figure 2.2 A simplified confusion matrix used in validation step. Adopted from Barsi et al. 2018

In the validation/evaluation step, we followed the accuracy estimation steps described in Olofsson et al. (2014), which yielded the area-adjusted overall accuracy (OA) estimate and its associated confidence interval for each map. The producer's accuracy (PA) of the map was calculated by dividing the correctly mapped change occurrences by the total number of change occurrences detected in the reference data (Barsi et al. 2018). On the other hand, the User's accuracy (UA) of the map was calculated by using the total number of reference points that coincided with the changes depicted in the map as the denominator (Barsi et al. 2018). PA depicts the sensitivity, while UA indicates the specificity of the produced maps (for more details see 3.2). The best mapping approach would be the one that produced a map with the highest overall accuracy, sensitivity, and specificity.

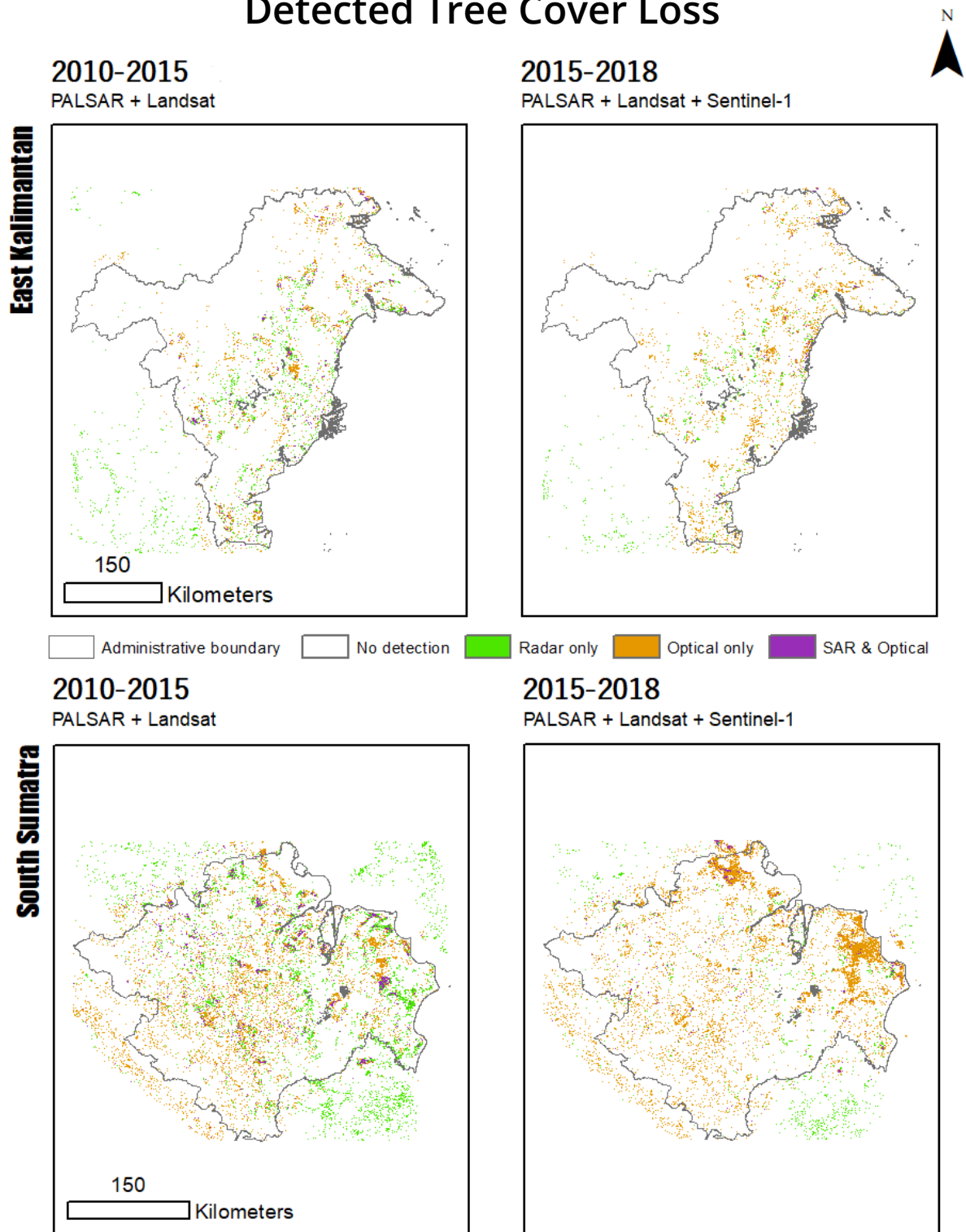# 3. Evaluation of the produced maps

Detected Tree Cover Loss

Figure 3.1 Detected changes in SS and EK in 2010-2015 and 2015-2018 periods

The produced maps (Figure 3.1) show the detected tree cover loss in EK and SS in the 2010-2015 and 2015-2018 periods. The distribution of the coloured "change" pixels indicates a very small agreement between the optic-based and the radar-based change maps, which may be related to the fact that the optical and radar sensors are sensitive to different properties of land covers. There was no clear pattern of the areas where the two maps agree and areas where the two disagree. It is worth noting that the major wildfire in Ogan Komering Ilir district in the eastern part of SS in 2015 (Dewi et al. 2015) was detected in the optic-based map but 'flew under the radar' in the radar-based change map.
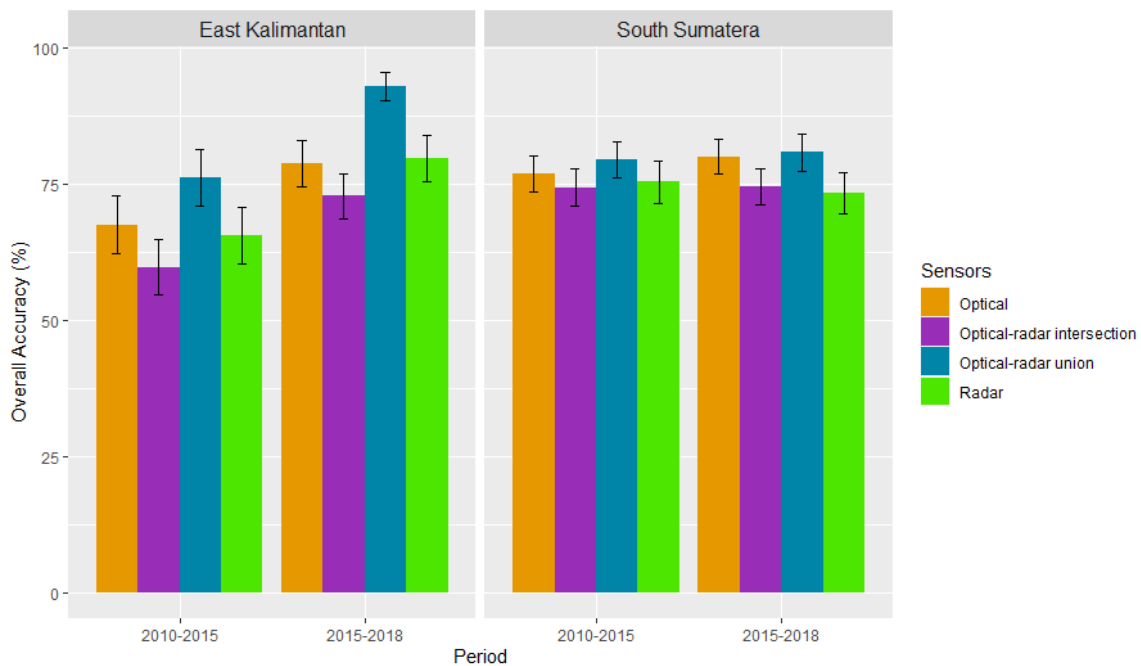
Figure 3.2 Area-adjusted overall accuracy values associated with the change maps derived from different approaches implemented in the analysis

3.1 Overall Accuracy

The change map derived by taking all of the changes detected by either the optic-based or radar-based change maps had the highest overall accuracy with the overall accuracy > 75% (Figure 3.2). This finding shows that the most accurate change detection can be obtained by combining the optical and radar approaches. Another takeaway from the results is that by itself, the optic-based change map outperformed the radar-based change map even though the two approaches had only moderate accuracies. The low accuracy of radar-based change maps might be associated with the higher noise content in radar data relative to the optical images despite the higher spatial resolution.

Figure 3.3 Producer's (PA) and User's accuracy (UA) of the produced maps

3.2 Producer's and User's Accuracy

In general, both the optic-based and radar-based change maps have low producer's accuracy (PA), which means that many changes that actually occurred, had been undetected (Figure 3.3). A combination of the two maps through a simple union increases the PA or the sensitivity. When 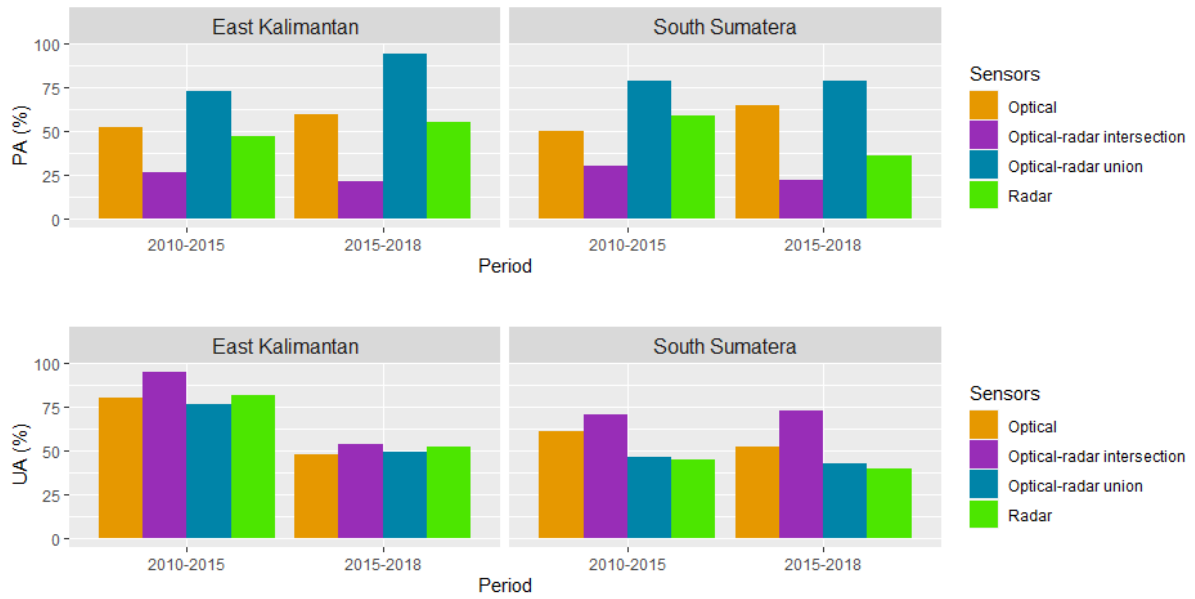we only considered the intersection between the optical- and radar-based maps, there was relatively lower PA. The optic-based change map has a slightly better capability in detecting the tree cover loss in EK. However, the results were different in SS. The two studied periods showed inconsistent results: in 2010-2015, the radar-based map had a slightly better sensitivity relative to the optic-based map; in 2015-2018, the optical-based map is more sensitive than the radar-based map. Further analysis is required to unveil the possible causes of the temporal variation.

Similar to PA, User's accuracy (UA) values also showed a difference between SS and EK (Figure 3.3). In SS, the optic-based map consistently had a higher UA level, or specificity, than the radar-based change map, while in EK, the radar-based map was superior to the optic-based map. The distinct results obtained from the two sites might suggest that the landscape features may affect the different sensor types' ability to tell the true change apart from the false positives (commission error). When we only considered the intersection between the optical- and radar-based maps, there was relatively lower commission error and, hence, higher UA. Therefore, when specificity is prioritized, the areas where both the optical and radar change maps agreed are most useful.

A more detailed look into the UA and PA of the produced maps is provided as confusion matrices in the Appendix: Confusion matrices.

4. Limitations & Recommendations

The results of our exploratory analysis provide an empirical review of the utilization of optical and radar satellites in detecting tree cover loss in tropical forest landscapes. Given the similar performance of the optic-based and radar-based mapping as well as the simpler preprocessing and processing steps in optic-based change mapping, tree cover loss detection using optical satellites appears to be a good option to monitor the studied landscapes. However, it should be noted that we expect different outcomes when other preprocessing and processing methods are implemented, e.g., by using a more sophisticated preprocessing (Small et al. 2021) or a more complex change detection algorithm (Durieux et al. 2019).

In general, we learned that a better mapping accuracy could be obtained by combining the optic-based map with the radar-based map. We only implemented a simple way of combining the two different sensor types in this work. However, more sophisticated approaches should be explored, for example, by fusing the optical and radar data using machine learning algorithms, like random forest (Breiman 2001).

Despite our best effort in interpreting the very-high resolution satellite data, some degrees of uncertainty was present in reference data collection. Many survey points did not have a clear image that allowed useful interpretation, and even when they did, some of them had substantial cloud cover. This situation limited the number of usable reference data in the validation process because reference points associated with low interpretation confidence were omitted. This limitation highlights the importance of ground-based surveys in filling the gap in reference data.

More systematic assessments are needed to explain the factors that cause the sensors to perform better in one context but not in other contexts. In addition, a more local-scale analysis at well-studied sites using different sets of input combinations is valuable in revealing the pros and cons of using different sensor types to detect tree cover loss under different biogeophysical contexts.

References

Barsi, Zs Kugler, I. László, Gy Szabó, and H. M. Abdulmutalib. 2018. "Accuracy Dimensions in Remote Sensing." *International Archives of the Photogrammetry, Remote Sensing and Spatial Information Sciences - ISPRS Archives* 42(3):61–67.

Bey, Adia, Alfonso Sánchez Paus Díaz, Danae Maniatis, Giulio Marchi, Danilo Mollicone, Stefano Ricci, Jean François Bastin, Rebecca Moore, Sandro Federici, Marcelo Rezende, Chiara Patriarca, Ruth Turia, Gewa Gamoga, Hitofumi Abe, Elizabeth Kaidong, and Gino Miceli. 2016. "Collect Earth: Land Use and Land Cover Assessment through Augmented Visual Interpretation." *Remote Sensing* 8(10):1–24.

Breiman, Leo. 2001. "Random Forests." *Machine Learning* 45:5–32.

Dewi, Sonya, Meine van Noordwijk, Adrian Dwiputra, Hesti L. Tata, Andree Ekadinata, Gamma Galudra, Niken Sakuntaladewi, and Atiek Widayati. 2015. *Peat and Land Clearing Fires in Indonesia in 2015: Lessons for Polycentric Governance*. Vol. 51. Nairobi.

Durieux, Alice M., Matthew T. Calef, Scott Arko, Rick Chartrand, Caitlin Kontgis, Ryan Keisler, and Michael S. Warren. 2019. "Monitoring Forest Disturbance Using Change Detection on Synthetic Aperture Radar Imagery." in *Proceedings of SPIE 1139, Applications of Machine Learning*. Vol. 1113916.

Gorelick, Noel, Matt Hancher, Mike Dixon, Simon Ilyushchenko, David Thau, and Rebecca Moore. 2017. "Google Earth Engine: Planetary-Scale Geospatial Analysis for Everyone." *Remote Sensing of Environment* 202:18–27.

Hansen, M. C., P. V. Potapov, R. Moore, M. Hancher, S. A. Turubanova, D. Thau, S. V. Stehman, S. J. Goetz, T. R. Loveland, A. Kommareddy, L. Chini, C. O. Justice, and J. R. G. Townshend. 2013. "High-Resolution Global Maps of 21st-Century Forest Cover Change." *Science* 342(6160):850–53.

Olofsson, Pontus, Giles M. Foody, Martin Herold, Stephen V. Stehman, Curtis E. Woodcock, and Michael A. Wulder. 2014. "Good Practices for Estimating Area and Assessing Accuracy of Land Change." *Remote Sensing of Environment* 148:42–57.

Sabins, Floyd F. 1997. *Remote Sensing: Principles and Interpretation*. 3rd ed. New York: W.H. Freeman and Co.

Small, David, Christoph Rohner, Nuno Miranda, Marius Ruetschi, and Michael E. Schaepman. 2021. "Wide-Area Analysis-Ready Radar Backscatter Composites." *IEEE Transactions on Geoscience and Remote Sensing* 1–14.

The Ministry of Environment and Forestry of Indonesia. 2021. "Indonesian National Carbon Accounting System." *Provincial Profile*. Retrieved (http://incas.menlhk.go.id/data/south-sumatra/).

Zhu, Zhe and Curtis E. Woodcock. 2014. "Continuous Change Detection and Classification of Land Cover Using All Available Landsat Data." *Remote Sensing of Environment* 144:152–71.

Appendix: Confusion matrices

The **overall accuracy (OA)** values provided below are not identical with the area-adjusted overall accuracy used in the main body of the report. OA values provided below were calculated without taking into account the area of each class within the study sites.

South Sumatera 2010-2015

Optical

Map\Ref	noChange	change	Sum	UA (%)
noChange	399	108	507	**78.7**
change	68	108	176	**61.36**
Sum	467	216	683	
PA (%)	**85.44**	**50**		OA = 74.23%

Radar

Map\Ref	noChange	change	Sum	UA (%)
noChange	310	88	398	**77.89**
change	157	128	285	**44.91**
Sum	467	216	683	
PA (%)	**66.38**	**59.26**		OA = 64.13%

Optical-radar union

Map\Ref	noChange	change	Sum	UA (%)
noChange	269	45	314	**85.67**
change	198	171	369	**46.34**
Sum	467	216	683	
PA (%)	**57.6**	**79.17**		OA = 64.42%

Optical-radar intersection

Map\Ref	noChange	change	Sum	UA (%)
noChange	440	151	591	**74.45**
change	27	65	92	**70.65**
Sum	467	216	683	
PA (%)	**94.22**	**30.09**		OA = 73.94%

South Sumatera 2015-2018

Optical

Map\Ref	noChange	change	Sum	UA (%)
noChange	367	73	440	**83.41**
change	119	133	252	**52.78**
Sum	486	206	692	
PA (%)	**75.51**	**64.56**		OA = 72.25%

Radar

Map\Ref	noChange	change	Sum	UA (%)
noChange	373	131	504	**74.01**
change	113	75	188	**39.89**
Sum	486	206	692	
PA (%)	**76.75**	**36.41**		OA = 64.74%

Optical-radar union

Map\Ref	noChange	change	Sum	UA (%)
noChange	271	44	315	**86.03**
change	215	162	377	**42.97**
Sum	486	206	692	
PA (%)	**55.76**	**78.64**		OA = 62.57%

Optical-radar intersection

Map\Ref	noChange	change	Sum	UA (%)
noChange	469	160	629	**74.56**
change	17	46	63	**73.02**
Sum	486	206	692	
PA (%)	**96.5**	**22.33**		OA = 74.42%

East Kalimantan 2010-2015

Optical

Map\Ref	noChange	change	Sum	UA (%)
noChange	191	94	285	**67.02**
change	25	104	129	**80.62**
Sum	216	198	414	
PA (%)	**88.43**	**52.53**		OA = 71.26%

Radar

Map\Ref	noChange	change	Sum	UA (%)
noChange	195	105	300	**65**
change	21	93	114	**81.58**
Sum	216	198	414	
PA (%)	**90.28**	**46.97**		OA = 69.57%

Optical-radar union

Map\Ref	noChange	change	Sum	UA (%)
noChange	173	54	227	**76.21**
change	43	144	187	**77.01**
Sum	216	198	414	
PA (%)	**80.09**	**72.73**		OA = 76.57%

Optical-radar intersection

	noChange	change	Sum	UA (%)
noChange	213	145	358	**59.5**
change	3	53	56	**94.64**
Sum	216	198	414	
PA (%)	**98.61**	**26.77**		OA = 64.25%

East Kalimantan 2015-2018

Optical

Map\Ref	noChange	change	Sum	UA (%)
noChange	250	61	311	**80.39**
change	101	92	193	**47.67**
Sum	351	153	504	
PA (%)	**71.23**	**60.13**		**OA = 67.86%**

Radar

Map\Ref	noChange	change	Sum	UA (%)
noChange	275	68	343	**80.17**
change	76	85	161	**52.8**
Sum	351	153	504	
PA (%)	**78.35**	**55.56**		**OA = 71.43%**

Optical-radar union

	noChange	change	Sum	UA (%)
noChange	202	9	211	**95.73**
change	149	144	293	**49.15**
Sum	351	153	504	
PA (%)	**57.55**	**94.12**		**OA = 68.65%**

Optical-radar intersection

	noChange	change	Sum	UA (%)
noChange	213	145	358	**59.5**
change	3	53	56	**94.64**
Sum	216	198	414	
PA (%)	**98.61**	**26.77**		**OA = 64.25%**